Monte-Carlo-based consequence analysis of nuclear accidents under extreme conditions

Shengyu LIU[1], Wei WANG[1]

[1] *Department of Mechanical Engineering, City University of Hong Kong, Kowloon Tong, Hong Kong, China*

ABSTRACT

The source term and meteorological conditions are key sources of uncertainty in assessing the consequences of severe nuclear accidents. However, previous studies have mainly focused on specific source terms and meteorological conditions. This study presents a Monte Carlo-based method that propagates both source term and meteorological uncertainties. The source term uncertainty is propagated by sampling from multiple source term categories (STCs), while the propagation of the meteorological data is by applying the randomized-start block sampling method to long-term meteorological data. Dispersion scenarios are established based on the samples of the source term and meteorological data. Then, the off-site consequence is evaluated based on the official dose conversion coefficient and corresponding measures. Validation of calculation accuracy is provided first by utilizing the release information of the Fukushima Daiichi nuclear accident and comparing calculation results with official data from the Japanese government. Then the method is applied to the Daya Bay Nuclear Power Plant (DBNPP). The findings reveal that the dispersion model can provide accurate calculation results, while the case study result of DBNPP shows a higher probability of serious consequences in the Southwest and Northeast directions around the nuclear power plant, due to the wind direction distribution.

Keywords: Uncertainty, Monte-Carlo Sampling; Radionuclide dispersion; Consequence assessment

I. INTRODUCTION

Worldwide expansion of Nuclear Power Plants (NPPs) has been accelerated recently [1]. Nevertheless, the risks that off-site release of radionuclides from severe nuclear accidents can create both acute and chronic impacts on public health. Recently, many studies have been dedicated to assessing the off-site consequences. Combinations of Emergency Planning Zones (EPZs) are developed to optimize consequence mitigation measures [2]. The off-site consequence is also investigated for the advanced power reactor 1400 (APR1400), where some specific possible accidents and corresponding meteorological conditions are covered to give a preliminary emergency framework [3]. However, uncertainty consideration is often inadequate in the off-site consequence assessment [4].

To assess the radioactive material dispersion and distribution that accounts for multiple uncertainties under severe nuclear accident conditions, the forward modelling methods offer a proactive way to comprehensively propagate main uncertainties related to both source terms and meteorological conditions [5]. Discrete source term categories (STCs) have been used to represent variability in release conditions, while some studies consider different source terms for a specific accident, resulting in not capturing the full range of possible source term variations, such as release magnitude [6]. The Level 2 PRA method is adopted to achieve more continuous and realistic source term distributions, such as release amount and duration [7]. Some other studies concentrate on the meteorological uncertainty. The ensemble method, which is developed for weather forecasting, shows better performance in the radionuclide dispersion than the traditional deterministic method by showing significant predictive rate accuracy improvement [8]. However, there are limited studies that fully combine the uncertainty propagation for both the source term and the meteorological data.

In this work, we propose a Monte Carlo-based (MC-based) consequence assessment method to fully combine these uncertainties, where the MC sampling approach is applied to both STCs and meteorological data. Then, dispersion scenarios are established, and consequence assessment is based on dose evaluation and emergency measures. The accuracy of the dispersion model is validated, and the results of the Daya Bay Nuclear Power Plant case study show a higher probability of serious consequences in the Southwest and Northeast directions around the nuclear power plant.

2. MATERIALS AND METHODS

In this part, mandatory data, including STCs and the meteorological data collection, will be given. Subsequently, the Monte-Carlo sampling method is used to sample from distributions of source term and meteorological data, while the

randomized-start block sampling approach is applied to long-term meteorological data. Finally, the off-site consequence evaluation process involving the dose conversion coefficient and corresponding measures will be demonstrated.

II.A. Monte-Carlo-based sampling

II.A.1. STCs collection

Consequently, discrete and hypothetical STCs are considered in this method. The technical report WASH-1400 provides STCs where the different STCs are contained [9]. The STCs presented in the report are obtained through the level 2 PSA estimation. The STCs are summarized in **TABLE I**. Besides, the core inventories and half-life of different radionuclides are summarized in **TABLE II**.

TABLE I. STCs and their corresponding release information

Release category	Probability (yr^{-1})	Relatively Probability	Release fraction of Core Inventory					Timing (hr.)	Duration (hr.)	Release height
			I-131	Cs-137	Xe-Kr	Te-132	Sr-90			
P1	9×10^{-7}	0.0018	0.7	0.4	0.9	0.4	0.05	2.5	0.5	25
P2	8×10^{-6}	0.016	0.7	0.5	0.9	0.3	0.06	2.5	0.5	0
P3	4×10^{-6}	0.008	0.2	0.2	0.8	0.3	0.02	5.0	1.5	0
P4	5×10^{-7}	0.001	0.09	0.04	0.6	0.03	5×10^{-3}	2.0	3.0	0
P5	7×10^{-7}	0.0014	0.03	9×10^{-3}	0.3	5×10^{-3}	1×10^{-3}	2.0	4.0	0
P6	6×10^{-6}	0.012	8×10^{-4}	8×10^{-4}	0.3	1×10^{-3}	9×10^{-5}	12.0	10.0	0
P7	4×10^{-5}	0.08	2×10^{-5}	1×10^{-5}	6×10^{-3}	2×10^{-5}	1×10^{-6}	10.0	10.0	0
P8	4×10^{-5}	0.08	1×10^{-4}	5×10^{-4}	2×10^{-3}	1×10^{-6}	1×10^{-8}	0.5	0.5	0
P9	4×10^{-4}	0.8	1×10^{-7}	6×10^{-7}	3×10^{-6}	1×10^{-9}	1×10^{-11}	0.5	0.5	0

TABLE II. Core Inventories and Half-lives of different radionuclides

Radionuclide	Core inventory (Curies)	Half-life (days)
I-131	8.5×10^{7}	8.05
Cs-137	4.7×10^{6}	11000
Te-132	1.2×10^{8}	3.25
Xe-133	1.7×10^{8}	5.28
Kr-88	6.8×10^{7}	0.117
Sr-90	3.7×10^{6}	11030

Studies have illustrated the reconstructed source term of the Fukushima nuclear accident, among which the longest period is from 2011/03/12 to 2011/05/01 [10]. Therefore, only situations where the release amount of both I and Cs exceeds that of the Fukushima Daiichi nuclear accident during this period are considered as severe accidents. The relative probability calculation formulation is shown in Eq. (1). The severe nuclear accident release categories and the results are listed in **TABLE III**.

$$\mathbf{P}_{r,i} = \frac{\mathbf{P}_{a,i}}{\sum_{i} \mathbf{P}_{a,i}} \tag{1}$$

where $\mathbf{P}_{a,i}$ and $\mathbf{P}_{r,i}$ represent the absolute probability and relative probability of release category i.

TABLE III. Relative probability of severe nuclear accident release categories

Release category	Probability (yr^{-1})	Relative Probability
P_1	9×10^{-7}	0.06383
P_2	8×10^{-6}	0.5674
P_3	4×10^{-6}	0.2837
P_4	5×10^{-7}	0.03546
P_5	7×10^{-7}	0.04964

In this case, the relative probability of each release category should be calculated by Eq. (1), where the results are shown in **TABLE III**.

II.A.2. Randomized-start block sampling

As mentioned before, the uncertainty caused by the weather temporal variation pattern is not considered in the ensemble and classification means. Therefore, in this work, long-term historical weather observation data will be collected, which is further combined with the terrain data to provide a long-term meteorological field. Then, the randomized-start block Monte Carlo sampling method will be utilized to cover the uncertainty. Assuming the meteorological data we collected forms a sample space Ω^M, where the hourly meteorological data for a specified period of time, assumed to be D days, is stored. Each hourly meteorological data is represented by d_j^M, where j represents the specific time point. Then we obtain the relationship:

$$\Omega^M = \left\{d_1^M, d_2^M, ..., d_p^M\right\}, p = 24D \tag{2}$$

In Formulation (2), the stored time period in the sample space includes all the hourly time point, which is varied from 1 to p. For instance, if the hourly meteorological data from the beginning hour of day 1 to the end hour of day N is sampled, then there will be $24N$ hourly data, and $j \in \{1, 2, ..., 24N\}$.

As soon as the data is collected, the randomized-start block sampling method is applied to the sample space Ω^M. A random hourly data is chosen to be the beginning of the meteorological sample, and with the specific meteorological time period, the meteorological sample will be extracted from the sample space, which is represented by M. For all the sample extracted from the sample space, we have:

$$\begin{aligned} &M_j \subseteq \Omega^M, j = 1, 2, ..., m \\ &M_j = \left\{d_q^M, d_{q+1}^M, ..., d_{q+24N-1}^M\right\}, 1 \le q \le p - 24N + 1 \end{aligned} \tag{3}$$

where j means the j[th] sampling. The beginning hour p in the sample is set to be less than $n - 24N + 1$ to avoid the last hourly meteorological data exceeding the last meteorological data in the sample space Ω^M.

Meteorological data is provided in many online sources, where the fifth generation of ECMWF reanalysis data (ERA5) is frequently used due to its data integrity [11]. In this work, the ERA5 reanalysis data is collected since it is more accurate and provides complete data for both surface and upper air meteorological data.

The MC sampling is applied to STCs to randomly sample a source term, while the meteorological data is sampled by using the randomized-start block sampling method. The source term and meteorological data generated from each sampling are combined to establish an uncertain dispersion scenario.

II.B. Dispersion model

Recently, different dispersion calculation models have been utilized to investigate radionuclide dispersion. The most used models are the Lagrangian model [6], the Gaussian plume model [12], and the Gaussian puff model [13]. Advantages and disadvantages exist in each dispersion model, and they are presented in TABLE IV. The Gaussian puff model is utilized in this work due to our assessment spatial range.

TABLE IV. Comparison of different dispersion models

Models	Advantages	Disadvantages
Lagrangian	Suitable for long-distance dispersion (Up to thousands of kilometers)	Computationally intensive
Gaussian plume	Costs little run time and small requirement of data input	Not accurate for mid-distance or long-distance (Larger than 30-50km)
Gaussian puff	Cost less time while keeping relatively accurate for mid-distance	Not as accurate as the Lagrangian model for long-distance calculation

The CALPUFF software, which adopts the Gaussian puff model, is used to simulate radionuclide dispersion, as it can model the radionuclide transportation under complex terrain.

II.C. Consequence analysis

The dose conversion coefficients are used to convert the concentration distribution to the dose distribution. Investigations have pointed out that inhalation contributes to the dose effect in the early dispersion of radionuclides, which is considered in this work, while the impacts of other routes are negligible. The effective dose conversion formulation in terms of inhalation is shown in Eq. (4)

$$E = \sum \left(e_i M C_i T \right) \tag{4}$$

where E is the effective dose or equivalent dose, i represents the species of the radionuclides, e is the effective dose coefficient for different radionuclides, M is the inhalation rate for adults, which is taken as 16 m^3/day, C is the concentration of radionuclides, and T represents the time period. The inhalation dose coefficients of these radionuclides [14,15] are presented in TABLE V.

TABLE V. Dose coefficient of different radionuclides

Radionuclide	Effective Dose Coefficient (Sv/Bq)
I-131	7.4×10^{-9}
Cs-137	4.6×10^{-9}
Te-132	1.8×10^{-9}
Xe-133	1.2×10^{-9}
Kr-88	8.4×10^{-9}
Sr-90	2.4×10^{-8}

In this work, we consider one dose criteria with its emergency measure, which are listed in TABLE VI.

TABLE VI. Dose criteria and corresponding measures

Dose level	Protective measures
50 mSv/week	Temporary evacuation

3. RESULTS AND DISCUSSIONS

III.A. Verification of the accuracy

A squared area with an edge length of 100 km is chosen, where its center is the Fukushima Daiichi nuclear power plant. The area is shown in FIGURE 1:

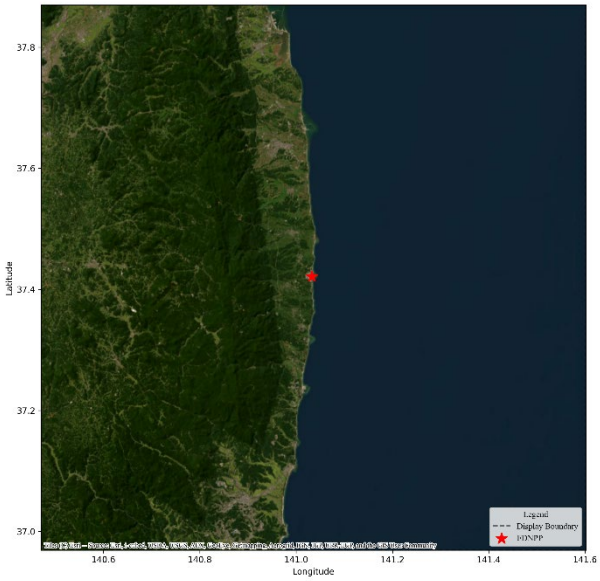

FIGURE 1. The calculation area of the Fukushima nuclear accident case

The source term of the Fukushima nuclear accident has been estimated by several recent studies. In this work, we adopted a rough estimation of the source term from 12/03/2011 to 01/05/2011 published in an early work [10].

The surface meteorological data is adopted from the ERA5 reanalysis dataset and the Japanese Reanalysis for Three-Quarters of a Century (JRA-3Q) data. The upper air meteorological data are adopted from the ERA5 reanalysis dataset. The upper air data provided by ERA5 is combined with both surface observation data of ERA5 and JRA-3Q, since it is more complete. Then, two kinds of meteorological data combinations, which are ERA5 surface-ERA5 upper and JRA-3Q surface-ERA5 upper, are used to calculate radionuclide dispersion. The average release rate of the source term and the time-phased release rate are both applied to calculate the radionuclide dispersion result.

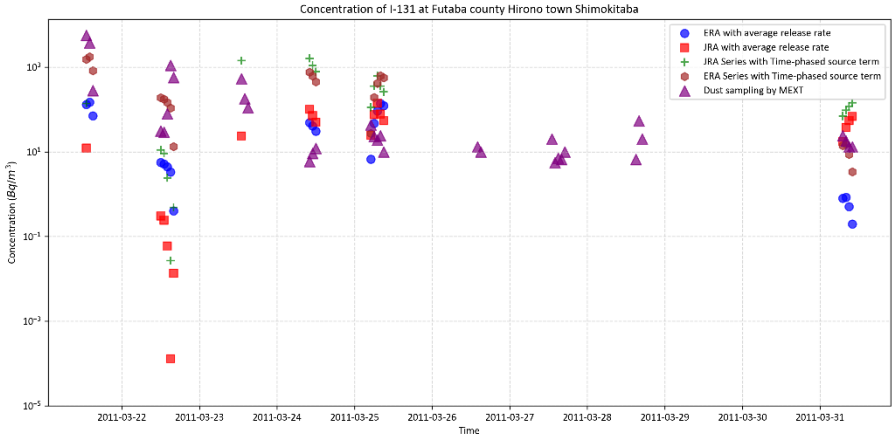

FIGURE 2. Comparison of calculation and dust sampling results

To verify the accuracy of the dispersion model, we compare the calculation results by using the combination of these two kinds of meteorological data, and the source term presented in [10], to the dust sampling result measured by the Ministry of Education, Culture, Sport, Science and Technology (MEXT) of Japan [16]. The dust sampling location is chosen to be Futaba County, Hirono town, Shimokitaba, since it provides an early and complete concentration of both I-131 and Cs-137. As shown in Figure 2, the concentration of radionuclides calculated by the average release rate in the early period is lower than that estimated by the time-phased release rate, which is due to the higher release rate in the early release period. There is no concentration result calculated by the simulation on some days, since there is no airborne concentration shown in these specific periods at this location. The result calculated by ERA5 surface-ERA5 upper and time-phased release rate is closest to the measured results, which are basically on the same order of magnitude. Therefore, the calculation accuracy of CALPUFF is verified. The ERA5 surface-ERA5 upper meteorological data combination will be adopted in the following verification of the method and the case study in Section 4.

III.B. Case Study: DBNPP

The Daya Bay nuclear power plant has been operating for some decades, and there are some population-dense cities around this nuclear power plant, such as Shenzhen and Hong Kong. Therefore, in this work, the Daya Bay nuclear power plant is chosen as the case study. The calculation area and the corresponding configurations of the calculation are listed in Table 7. The surface and upper air meteorological data are provided by the ERA5 reanalysis dataset as a result of the verification in Section 3.1. As mentioned previously, each meteorological data point contains both surface and upper air data, and the locations of these data points are shown in Table 7.

TABLE VII. Configuration of the dispersion case at the Daya Bay nuclear power plant

Variables	Values
Calculation area	200 km×200 km UTM: 50N, X: 147.413-347.413 km; Y: 2401.099-2601.099 km Longitude-Latitude: 21.678334°-23.512949° N 113.593252°-115.505487° E
Grid size	2 km
Number of meteorological data points	4×4 (The distance between each meteorological data point is 0.5°. The data point with the minimum latitude and longitude is located at

	21.93° N, 113.63° E, i.e., the lower left side of **FIGURE 3**)
Time range of the meteorological dataset	2005/01/01-2024/12/31
Radionuclide dispersion time in a single scenario	7 days
Number of Scenarios	5000

After setting the configurations and calculating each dispersion scenario, the radionuclide concentration results are obtained. The surface 7-day-average concentration results of I-131 in different dispersion scenarios are calculated. For each scenario, the distributions of the radionuclide are different due to the different meteorological conditions. In these dispersion scenarios, the calculated concentration coverage range of some scenarios is relatively large, while the concentration coverage range of other scenarios is concentrated in a particular direction. The large concentration coverage range is due to the significant change in wind direction in this scenario. In contrast, for the scenario where the wind direction is concentrated in a specific direction, the concentration coverage range is small. The dispersion trends of the different radionuclide species are the same due to the same configuration and the dispersion properties of these radionuclides. The concentration values of different radionuclides are different due to their different release amounts.

By applying the dose conversion coefficient introduced in Section 2, the surface concentration distributions of different radionuclides are converted to the dose distribution. Then, the dose value distributions in different directions under each dispersion scenario with Daya Bay Nuclear Power Station as the center are statistically analyzed, and the dose value distribution at each distance in each direction is statistically analyzed. In this case, directions are taken every 10°, and 36 directions are adopted. Moreover, for each direction, starting from the nuclear power plant, statistical points are taken outward every two kilometers (equal to the grid size). The dose values are sorted from small to large, and the 95% quantile is taken as the upper limit of the 95% confidence interval of the distribution. This upper limit indicates that when an accident occurs, there is a 95% confidence that the dose value will not exceed this upper limit. As the upper limit of the dose confidence interval at a certain distance in this direction exceeds the dose threshold corresponding to the evacuation listed in Section 2, the location is marked as a hazardous location that people should evacuate in the early stage of the accident without any other source of information.

As shown in Figure 3, the risky areas in terms of the evacuation measure are divided. The red area is calculated with the same release amount as that of the Fukushima Daiichi nuclear accident from 2011/03/12 to 2011/05/01, and the blue shadow area is divided by the calculation with scenarios sampled from the STCs and meteorological data. The land part of the risk area is cropped. However, due to the accuracy limitation of the land boundary line used for clipping, there are some slight differences between the clipped areas and the land areas shown in Figure 3. Nevertheless, this does not affect the analysis of the evacuation risk areas.

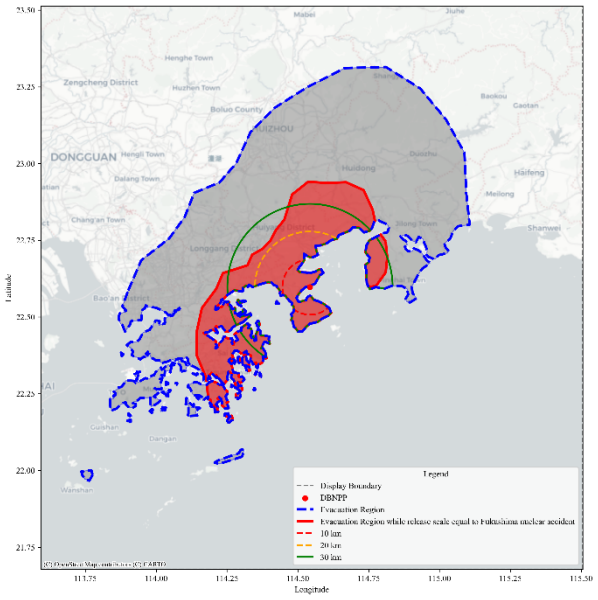

FIGURE 3. The spatial distribution of off-site consequences that indicates the evacuation necessity (Red: release amount equal to that of the Fukushima Daiichi nuclear accident from 2011/03/12 to 2011/05/01; Blue: release amounts are sampled from the release categories)

The spatial distribution of off-site consequences shown in FIGURE 3 indicates that when the release amount is equal to that of the Fukushima Daiichi nuclear accident, the evacuation area will exceed 30 km in most directions except the direction at the West-Northwest-North range. Similarly, the hazardous area calculated by the release amount sampled from the release categories shows that the risky area covers a wider area in the Northeast-Southwest direction, while that in the Northwest direction covers less than in other directions. This is due to the wind direction distributions at each meteorological data point. As depicted in FIGURE 4, the wind rose diagrams of each surface meteorological data point from 2005-2024 are calculated. For each data point, it is easily observed that most wind directions are distributed in the North-Northeast-East direction, and some wind directions are distributed in the South-Southwest direction. The dominant wind directions are North and Northeast. Therefore, most of the land area of Hong Kong, which is in the southwest direction of the Daya Bay nuclear power plant, will be affected with a relatively high probability under severe nuclear accident conditions. Besides, some land areas of Shenzhen and Huizhou will be affected with a high probability, too.

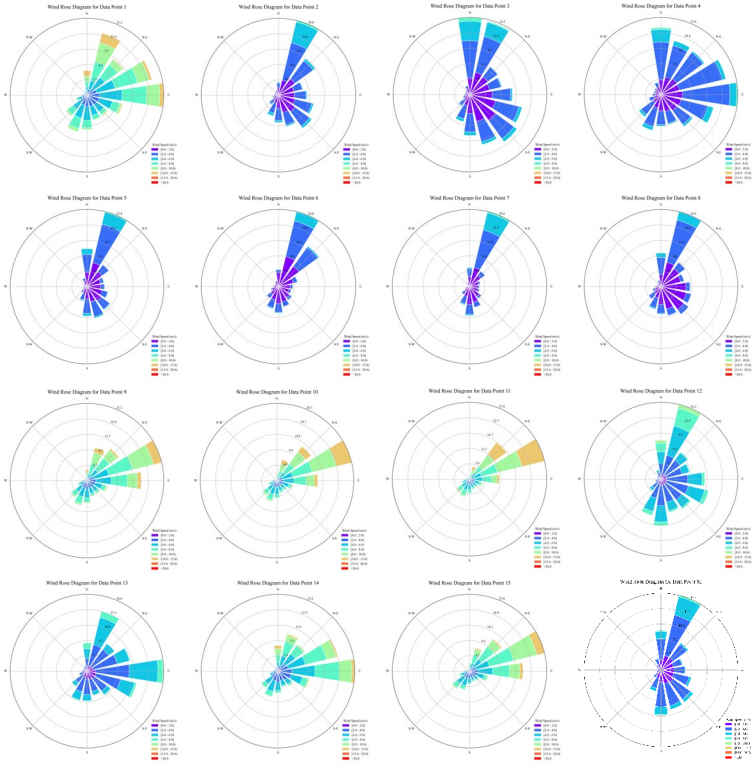

FIGURE 4. Wind rose diagrams of each surface meteorological data point from 2005-2024

II. CONCLUSIONS

In this work, A Monte-Carlo-based sampling method is proposed to combine the uncertainty propagations of the source term and meteorological data, where dispersion scenarios and consequence assessment are conducted based on source term and meteorological data samples. The conclusions of this work are summarized below:

1. Validation conducted by comparing the calculation results to the dust sampling data issued by the Japanese government shows that the model provides accurate calculation results.

2. A higher probability of serious consequences is shown in the Southwest and Northeast directions around the DBNPP, due to the wind direction distribution.

ACKNOWLEDGMENTS

The authors gratefully acknowledge the financial supports of this work by the Research Grants Council (RGC) of Hong Kong under the grant No. 11215323, and the National Natural Science Foundation of China under the grant No. 72101221.

REFERENCES

[1] J. PORTUGAL-PEREIRA, M. ESTEBAN, K. ARAÚJO, "Exposure of future nuclear energy infrastructure to climate change hazards: A review assessment", Energy Strategy Reviews, 53, 101365 (2024).
[2] M. KIMURA, OGURI ,TOMOMI, ISHIKAWA ,JUN, M. AND MUNAKATA, "Development of an evaluation method for planning of urgent protection strategies in a nuclear emergency using a level 3 probabilistic risk assessment", Journal of Nuclear Science and Technology 58, 278–291 (2021).
[3] I.A. ALRAMMAH, "Analysis of nuclear accident scenarios and emergency planning zones for a proposed advanced power reactor 1400 (APR1400)", Nuclear Engineering and Design 407, 112275 (2023).
[4] T. ZHOU, M. MODARRES, E.L. DROGUETT, "Multi-unit nuclear power plant probabilistic risk assessment: A comprehensive survey", Reliability Engineering & System Safety 213, 107782 (2021).
[5] S.J. LEADBETTER, S. ANDRONOPOULOS, P. BEDWELL, K. CHEVALIER-JABET, G. GEERTSEMA, F. GERING, T. HAMBURGER, A.R. JONES, H. KLEIN, I. KORSAKISSOK, A. MATHIEU, T. PÁZMÁNDI, R. PÉRILLAT, CS. RUDAS, A. SOGACHEV, P. SZÁNTÓ, J.M. TOMAS, C. TWENHÖFEL, H. DE VRIES, J. WELLINGS, "Ranking uncertainties in atmospheric dispersion modelling following the accidental release of radioactive material", Radioprotection 55, S51–S55 (2020).
[6] M. ULIMOEN, E. BERGE, H. KLEIN, B. SALBU, O.C. LIND, "Comparing model skills for deterministic versus ensemble dispersion modelling: The fukushima daiichi NPP accident as a case study", Science of The Total Environment 806, 150128 (2022).
[7] J.H. SØRENSEN, J. BARTNICKI, A.M. BLIXT BUHR, H. FEDDERSEN, S.C. HOE, C. ISRAELSON, H. KLEIN, B. LAURITZEN, J. LINDGREN, F. SCHÖNFELDT, R. SIGG, "Uncertainties in atmospheric dispersion modelling during nuclear accidents", Journal of Environmental Radioactivity 222, 106356 (2020).
[8] L. SHENG, Z. SONG, J. HU, K. LÜ, H. TONG, B. LI, Q. QIAO, "The comparison of ensemble or deterministic dispersion modeling on global dispersion during fukushima dai-ichi nuclear accident", Sci. China Earth Sci. 58, 356–370 (2015) .
[9] NUREG-75/014, "reactor safety study, an assessment of accident risks in U.S. commercial nuclear power plants, appendix VI."
[10] H. TERADA, G. KATATA, M. CHINO, H. NAGAI, "Atmospheric discharge and dispersion of radionuclides during the fukushima dai-ichi nuclear power plant accident. Part II: Verification of the source term and analysis of regional-scale atmospheric dispersion", Journal of Environmental Radioactivity 112, 141–154 (2012) .
[11] HERSBACH, H., BELL, B., BERRISFORD, P., BIAVATI, G., HORÁNYI, A., MUÑOZ SABATER, J., NICOLAS, J., PEUBEY, C., RADU, R., ROZUM, I., SCHEPERS, D., SIMMONS, A., SOCI, C., DEE, D., THÉPAUT, J-N., "ERA5 hourly data on single levels from 1940 to present. Copernicus Climate Change Service (C3S) Climate Data Store (CDS)", (2023)
[12] H. TERADA, H. NAGAI, K. TSUDUKI, A. FURUNO, M. KADOWAKI, T. KAKEFUDA, "Refinement of source term and atmospheric dispersion simulations of radionuclides during the fukushima daiichi nuclear power station accident", Journal of Environmental Radioactivity 213, 106104 (2020).
[13] J. CAI, K.F. IP, C. EZE, J. ZHAO, J. CAI, H. ZHANG, "Dispersion of radionuclides released by nuclear accident and dose assessment in the greater bay area of China", Annals of Nuclear Energy 132, 593–602 (2019) .
[14] "Age-dependent doses to members of the public from intake of radionuclides. 4: Inhalation dose coefficients", Pergamon Press, Oxford, (1996).
[15] K. ECKERMAN, J. HARRISON, H.-G. MENZEL, C.H. CLEMENT, "ICRP publication 119: Compendium of dose coefficients based on ICRP publication 60", Annals of the ICRP 41, 1–130 (2012).
[16] https://radioactivity.nra.go.jp/cont/en/results/land/dust-soil/beyond-20km-dust/dust%20sampling_All%20Results%20for%20May%202011.pdf